J. of Korean Oil Chemists' Soc.,
Vol. 32, No. 3. September, 2015. 451~460
ISSN 1225-9098 (Print)
ISSN 2288-1069 (Online)
http://dx.doi.org/10.12925/jkocs.2015.32.3.451



# Electrochemical and Raman Spectroscopy Analysis for D- and L-Tryptophan-*b*-Cyclodextrin Inclusion Complexes

Yu-Ra Jeong · So-Ra Lee · Pyeong-Soo Son · Seong-Ho Choi†

† *Department of Chemistry, Hannam University, Daejeon 305-811, Republic of Korea*
*(Received July 28, 2015; Revised August 17, 2015; Accepted September 10, 2015)*

**Abstract** : An enantioselective recognition of D- and L-tryptophan (Trp)-*b*-cyclodextrin (CD) inclusion complex was performed using electrochemical and FT-Raman spectroscopic analysis. From the electrochemical analysis, the selectivity coefficient ($K_{DL}$) of b-CD inclusion complexes was found higher than that of the D- and L-Trp in phosphate buffered saline (PBS, pH=7.0) solution. The percentage of enantioselectivity ($I_{\%ee}$) for peak current of D-Trp-b-CD inclusion complexes was observed higher than that of L-Trp-b-CD inclusion complexes in PBS solution. From Raman spectroscopy, chemical shift difference (D, $cm^{-1}$) for the C=C stretch, ring vibration, and ring breathing of D-Try-b-CD inclusion complex were observed higher than that of L-Trp-b-CD inclusion complex. The electrochemical and Raman spectroscopic analyses were found very useful for chiral detection of racemic amino acid in the presence of b-CD.

*Keywords : Electrochemical analysis, Raman spectroscopy analysis, D- and L-Tryptophan, b-Cyclodextrin inclusion complexes*

## 1. Introduction

Chirality is not only a fundamental chemical property of the optically active materials in nature, but also a critical factor in living systems [1]. The enantiomers of a chiral molecule may exhibit different biological activities. For instance, one of the enantiomer is very effective, while the other may be ineffective or even cause serious sides-effects for biomedical applications [2]. Therefore, development of the analytical methods for the enantioselective recognition of enantiomers is important in the fields of pharmaceuticals and biotechnology. There are various methods that have been employed for chiral analysis, including high performance liquid chromatography (HPLC) [3-5], capillary electrophoresis (CE) [6], chiral ligand exchange chromatography (CLEC) [7], fluorescence detection [8,9], molecular imprinting techniques [10], and electrochemical methods [11]. Among these approaches, electrochemical methods have attracted a lot of attentions owing to the advantages of low cost, high sensitivity, and simplicity.

Cyclodextrins (CDs) are cyclic natural oligomers connecting six, seven, and eight glucose units via $\alpha$-(1,4)-linkages, which are called $\alpha$-, $\beta$-, and $\gamma$-cyclodextrins, respectively. Schematically, the shape of CDs

†Corresponding author
(E-mail: shchoi@hnu.kr)

can be presented as a truncated cone with six, seven, and eight primary hydroxyl groups attached to the smaller opening cone while the remaining twelve, fourteen, and sixteen secondary hydroxyl groups are located on the larger opening of the cone [12,13]. As a consequence of these structural features, CDs are capable of forming inclusion complexes, even with molecules significantly larger than their cavities, providing at least some part of the guest can penetrate into the cavity [14,15]. CDs are known to be good models for enzymatic action, combining the cage effects with the conformational control of the guest molecule. Their stereoselective action, especially of $\alpha$- and $\beta$-CDs, offers new possibilities in particular for pharmaceutical application, e.g., enhancement of the bioavailability of certain drugs [16-18].

In our previous study, we prepared inclusion complexes of nitrophenols [19], Loxoprofen as a non-steroidal anti-inflammatory drug [20], and chlorostyrenes [21] with cyclodextrins as inclusion complex. Raman spectroscopy was used for their analysis and that remarkably exhibited Raman shifts due to the ring vibration of the molecule. However, there are not enough study about enantioselective recognition for the inclusion complexes using cyclodextrins in the solid state by using FT-Raman spectroscopy and electrochemical analysis. On the other hand, amino acids and their derivatives are important components in the chemical and biological systems [22]. Generally, different configurations of amino acids have different roles in the living system. L-Amino acids are used in the synthesis of proteins, while some D-amino acids are not participated in proteins synthesis or even generate adverse reaction to living organisms. Tryptophan (Trp) is an essential constituent of proteins and precursor of the neurotransmitter serotonin [23]. The level of Trp in plasma is closely related to the extent of hepatic disease [24]. L-Trp, which is called the second amino acid, is an important metabolite in human and animals. The imbalance or deficiency of L-Trp may cause several chronic diseases. Therefore, the enantioselective recognition of Trp enantiomers has become extraordinarily important.

In this study, we incorporated the D- and L-Trp on the b-CD in PBS solution (pH=7.0) in order to know enantioselective recognition by electrochemical analysis. Inclusion complex of D- and L-Trp with b-CD in the solid state was prepare for know enantioselective recognition by Raman spectroscopy. Based on the analysis results, the enantioselective recognition of inclusion complex was also discussed.

## 2. Experimental

### 2.1. Materials

D,L-tryptophan (Trp) and *b*-cyclodextrin (CD) inclusion complex were purchased from Sigma-Aldrich (Korea). Phosphate buffered saline solution (PBS, pH=7.0) was prepared by mixing of $NaH_2PO_4$ and $Na_2HPO_4$. Glassy carbon electrode (MF-2012) was purchased from Bioanalytical Systems, Inc. (U.S.A.). Ag/AgCl (012167 Ag/AgCl for reference electrode) was obtained from ALS Co., Ltd. (Japan). All other chemicals used in this study were analytical grade. A Millipore purification system (Millipore, MA, USA) was used for the purification of water.

### 2.2. Characterization

Cyclic voltagrams (CV) for inclusion complexes were obtained from Versa STAT 3 potentiostat/galvanostat (AMETEK PAR, USA) with conventional three-electrode system such as composite-coated glassy carbon (diameter, 3.0 mm) working electrode, a platinum wire counter electrode, and an Ag/AgCl (saturated KCl) as a reference electrode (Korea). Raman spectroscopy with High Resolution Raman was performed by LabRAM HR-800 (Horiba Jobin Yvon Inc., France).

## 3. Results and Discussion

### 3.1. Electrochemical analysis of L- and D-Trp-β -CD inclusion complexes

Fig. 1 shows the cyclic voltammograms (CVs) of the L- and D-Trp with $1.0 \times 10^{-4}$ M on GCE in 0.1 M PBS (pH=7.0) solution with a scan rate of 60 mV $s^{-1}$. A redox response of the L-Trp was observed with three oxidation peaks at 0.131, 0.394 and 0.724 V along with three reduction peaks at −0.701, −0.459 and −0.069 V. Here, the redox response of the L- and D- Trp with different concentration was found entirely in the same patterns. The detection limits for L- and D-Trp in PBS electrolyte was observed $1.0 \times 10^{-7}$ M. On the other hand, the electrochemical response for L- and D-Trp-b -CD inclusion complex was appeared entirely same pattern, but the peak current (mA) was smaller than that of the L- and D-Trp in PBS solution.

Fig. 2 shows the calibration curves for L- and D-Trp in CV with different concentration and scan rate at 0.131 V. Here, we found the linear calibration curves for both L- and D-Trp on the GC electrodes up to their concentrations in the range of $1.0 \times 10^{-2}$ M ~ $1.0 \times 10^{-6}$ M. Furthermore, the peak current for L-, and D-Trp at a scan rate of 60 mV $s^{-1}$ was observed higher than that of L- and D-Trp in CV at a scan rate of 30 mV $s^{-1}$. These results indicated that the redox reaction of L- and D-Trp was the reversible process onto the surface of GC electrode in PBS solution.

Fig. 3 exhibits the calibration curves for L-Trp and L-Trp-b-CD inclusion complex in PBS solution (pH = 7.0) at 0.131 V with different scan rates. It was also found that the calibration curves of L-Trp-b-CD inclusion complex was linear dependent on their

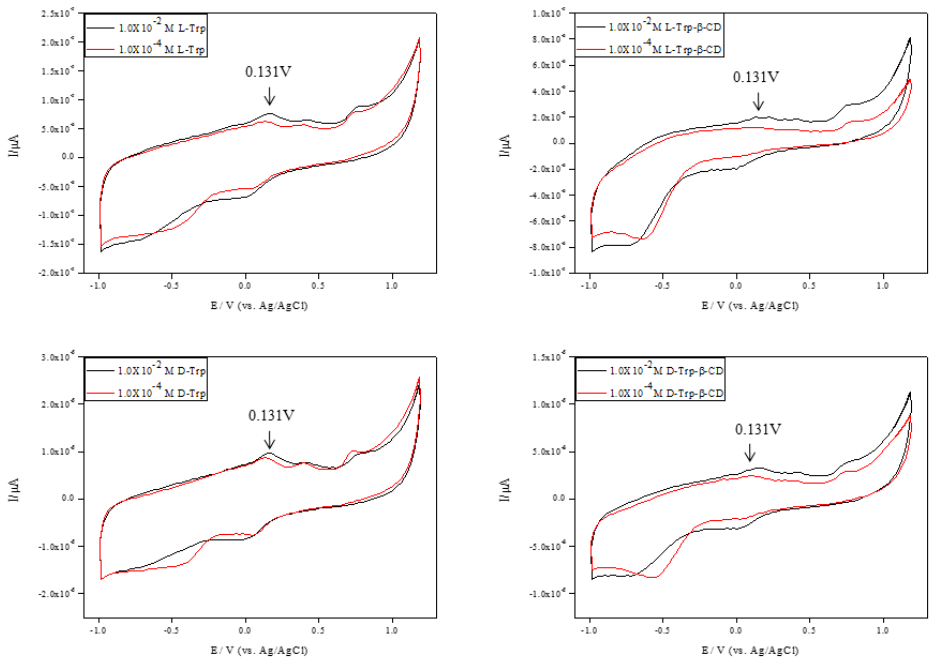


Fig. 1. Cyclic voltammograms of L-Trp and D-Trp on GCE in 0.1 M PBS (pH=7.0) with a scan rate 60 mV $s^{-1}$.

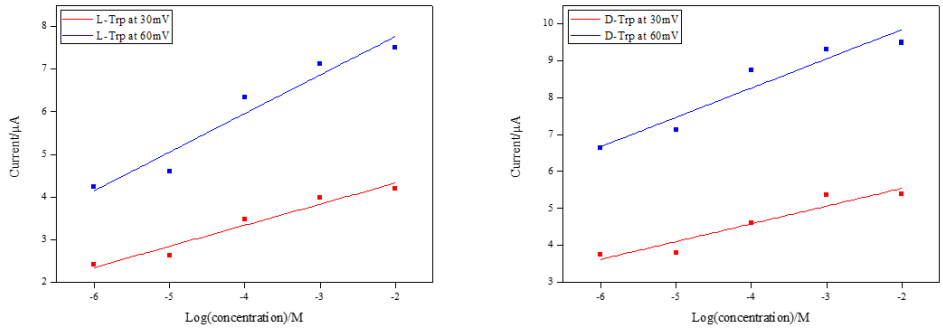


Fig. 2. Calibration curves of L-Trp and D-Trp at the 0.131n V point in 0.1 M PBS (pH=7.0) solution.

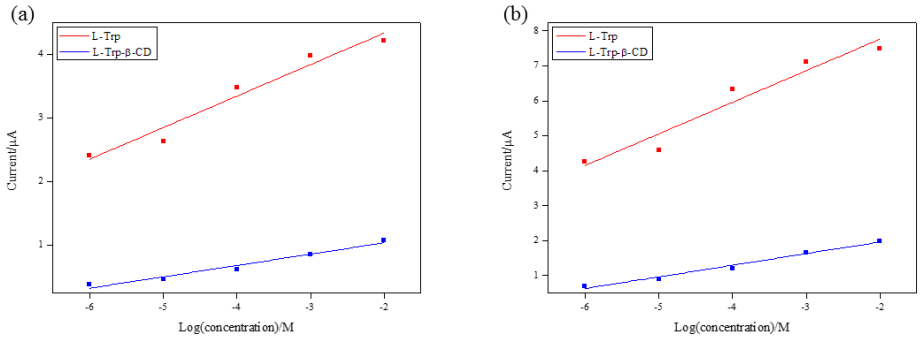


Fig. 3. Calibration curve for L-Trp and $\beta$-CD inclusion complex with L-Trp in 0.1 M PBS (pH=7.0) at 0.131 V. (a) with a scan rate of 30 mV s-1 and (b) with a scan rate 60 mV $s^{-1}$.

concentrations in the range of $1.0\times10^{-2}$ M ~ $1.0\times10^{-6}$ M, while the oxidation peak currents of the b-CD-L-Trp inclusion complex was lower than that of L-Trp. Here, the L-Trp as gust molecules could not approach onto the surface of GC electrode due to hindrance of b-CD as host molecules. At 0.1306 V point, we clearly observed higher value of the peak current in CV with a scan rate of 60 mV $s^{-1}$ for all active compounds than that of CV with a scan rate of 30 mV $s^{-1}$. This indicated that the redox reaction onto the surface of the GC electrode in PBS solution with active compounds was reversible.

Fig. 4 shows the calibration curves for D-Trp and D-Trp-b-CD inclusion complex in PBS electrolyte (pH = 7.0) at 0.131 V point at different concentrations and scan rates. The calibration curves of D-Trp-b-CD inclusion complex was also found liner dependent on their concentrations in the range of $1.0\times10^{-2}$M~$1.0\times10^{-6}$M.Whilethepeakcurrentsf orD-Trp-b-CD inclusion complex was lower than that of L-Trp in CV at 0.131 V point due to the blocking of b-CD as host compound to the surface of GC electrode in PBS solution.

Table 1 exhibits the peak current (I, mA) at 0.131 V point, selectivity coefficient, and the percentage of enantioselectivity at the peak

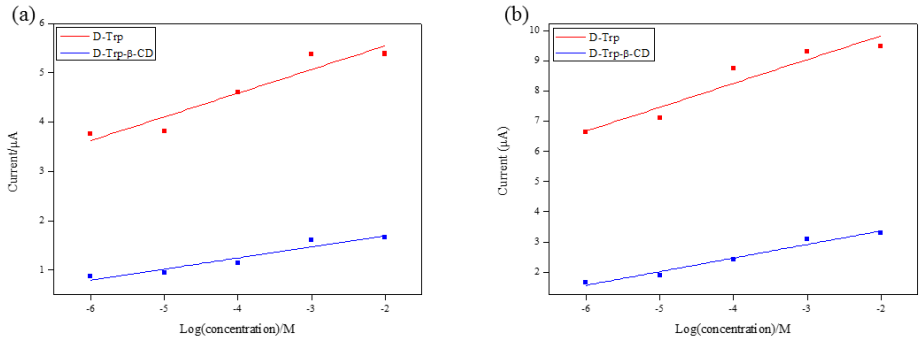


Fig. 4. Calibration curve for D-Trp and β-CD inclusion complex with D-Trp in 0.1 M PBS (pH=7.0) at 0.1306 V. (a) with a scan rate of 30 mV s-1 and (b) with a scan rate 60 mV $s^{-1}$.

current ($I_{\%ee}$) for the active compounds. Here, the selectivity coefficient for active compounds ($K_{DL}$) to GC electrode is calculated from the following equation [25]:

$$K_{DL}=(I_D/C_D)/(I_L/C_L) \quad (1)$$

Where $I_D$ and $I_L$ are the peak currents of D- and L-Trp, respectively; $C_D$and $C_L$ are the concentrations of the corresponding enantiomers. As shown in Table 1, the selectivity coefficient for L- and D-Trp was lower than that of the b-CD inclusion complexes. Furthermore, the selectivity coefficient for L-, D-Trp, and b-CD- inclusion complexes was increased with decreasing concentration. It is very interesting because the dissolved L- and D-Trp have the strong ionic property in PBS (pH=7.0) solution than the dissolved b-CD inclusion complexes. From these phenomena, the electrostatic repulsion of the dissolved L- and D-Trp exhibited to the surface of GC electrode than that of b-CD inclusion complexes.

On the other hand, the percent enantioselectivity ($I_{\%ee}$) for peak current of enantiomers was calculated from the following equation:

$$I_{\%ee}=I_D/I_D+I_L \quad (2)$$

where $I_D$ and $I_L$ are the peak currents of enantiomers. As you can see in Table 1, $I_{\%ee}$valuestoD-Trp-b-CD inclusion complexes was higher than that of L-Trp-b-CD inclusion complexes. This means that the chiral detection could be performed via redox peak currents of electrochemical analysis in the presence of b-CD as a host compound.

Table 2 shows the results of electrochemical analysis for L-, D-Trp and β-CD inclusion complexes by CV with a scan rate of 60 mV $s^{-1}$ in 0.1 M PBS (pH=7.0) solution. Here, the peak currents of D- and L- Trp were increased with increasing the scan rate (see, Table 1). The selectivity coefficient of b-CD inclusion complexes was higher than that of L- and D-Trp because the dissolved L- and D-Trp have the strong anionic property, while the dissolved b-CD inclusion complexes have the weak anionic properties to GC working electrode in PBS solution. $I_{\%ee}$ values to D-Trp-b-CD inclusion complexes was also found higher than that of L-Trp-b-CD inclusion complexes. This means that the chiral recognition in the presence of chiral b-CD as host compound could be determined via redox peak currents of electrochemical analysis.

Table 1. Electrochemical analysis for L-Trp, D-Trp and β-CD inclusion complexes by CV with a scan rate of 30 mV $s^{-1}$ in 0.1 M PBS (pH=7.0) solution

| | L- and D-Trp (at 0.131 V) | | | | β-CD inclusion complex (at 0.131 V) | | | |
|---|---|---|---|---|---|---|---|---|
| Concentration (M) | $I_{L\text{-}Trp}$ | $I_{D\text{-}Trp}$ | $K_{DL}=(I_D/C_D)/(I_L/C_L)$ | $I_{\%ee}=(I_D\text{-}I_L/(I_D+I_L)\times100$ | $I_{L\text{-}Trp\text{-}\beta\text{-}CD}$ | $I_{D\text{-}Trp\text{-}\beta\text{-}CD}$ | $K_{DL}=(I_D/C_D)/(I_L/C_L)$ | $I_{\%ee}=(I_D\text{-}I_L/(I_D+I_L)\times100$ |
| $1.0\times10^{-2}$ | 4.2055 | 5.3808 | 1.2794 | 12.260 | 1.0781 | 1.6646 | 1.5440 | 21.384 |
| $1.0\times10^{-3}$ | 3.9785 | 5.3673 | 1.3490 | 14.860 | 0.8594 | 1.5977 | 1.8529 | 30.047 |
| $1.0\times10^{-4}$ | 3.4768 | 4.6055 | 1.3246 | 13.965 | 0.6204 | 1.1349 | 1.8293 | 29.311 |
| $1.0\times10^{-5}$ | 2.6315 | 3.8037 | 1.4454 | 18.215 | 0.4702 | 0.9496 | 2.0196 | 33.765 |
| $1.0\times10^{-6}$ | 2.4064 | 3.7608 | 1.5403 | 21.961 | 0.3827 | 0.8689 | 2.2706 | 38.846 |

Table 2. Electrochemical analysis for L-Trp, D-Trp and β-CD inclusion complexes by CV with a scan rate of 60 mV $s^{-1}$ in 0.1 M PBS (pH=7.0) solution

| | L- and D-Trp (at 0.131 V) | | | | β-CD inclusion complex (at 0.131 V) | | | |
|---|---|---|---|---|---|---|---|---|
| Concentration (M) | $I_{L\text{-}Trp}$ | $I_{D\text{-}Trp}$ | $K_{DL}=(I_D/C_D)/(I_L/C_L)$ | $I_{\%ee}=(I_D\text{-}I_L/(I_D+I_L)\times100$ | $I_{L\text{-}Trp\text{-}\beta\text{-}CD}$ | $I_{D\text{-}Trp\text{-}\beta\text{-}CD}$ | $K_{DL}=(I_D/C_D)/(I_L/C_L)$ | $I_{\%ee}=(I_D\text{-}I_L/(I_D+I_L)\times100$ |
| $1.0\times10^{-2}$ | 7.5020 | 9.4858 | 1.2644 | 11.996 | 1.9929 | 3.2995 | **1.6556** | **24.688** |
| $1.0\times10^{-3}$ | 7.1168 | 9.3085 | 1.3080 | 13.343 | 1.6588 | 3.0799 | **1.8567** | **29.989** |
| $1.0\times10^{-4}$ | 6.3328 | 8.7441 | 1.3808 | 15.993 | 1.2077 | 2.4211 | **2.0047** | **33.438** |
| $1.0\times10^{-5}$ | 4.5901 | 7.1198 | 1.5511 | 21.603 | 0.9069 | 1.8794 | **2.0723** | **34.902** |
| $1.0\times10^{-6}$ | 4.2454 | 6.6242 | 1.5603 | 21.885 | 0.7025 | 1.6447 | **2.3406** | **40.141** |

### 3.2. Raman spectroscopy analysis L- and D-β -CD inclusion complexes

The hydrophobic properties of b-CD is useful for the incorporation in the indole, benzo[b]pyrrole, site of L- and D-Trp. Fig. 5 shows the FT-Raman spectra of L-Trp and L-Trp-b-CD inclusion complexes, in the 1480-1580 $cm^{-1}$, 1200-1280 $cm^{-1}$, and 1060-1180 $cm^{-1}$ regions, at room temperature. We selected above regions because the phenyl C=C stretching peak ν(C=C), ring vibration peak, and the ring breathing peaks of L-Trp and L-Trp-b-CD inclusion complexes have no interfering bands of the b-CDs. The pure L-Trp gives the characteristic phenyl ν(C=C) peak at 1557 $cm^{-1}$. The characteristic peaks of ring vibration and ring breathing for pure L-Trp were at 1232 $cm^{-1}$ and 1119 $cm^{-1}$,

respectively. After the inclusion of L-Trp to b-CD, the characteristic peaks were not shifted (see, Table 3).

Fig. 6 exhibits the FT-Raman spectra of D-Trp and D-Trp-b-CD inclusion complexes, in the 1480-1580 $cm^{-1}$, 1200-1280 $cm^{-1}$, and 1060-1180 $cm^{-1}$ region, at room temperature. The pure D-Trp gives the characteristic phenyl $\nu$(C=C) peak at 1557 $cm^{-1}$, whereas in the D-Trp-b-CD complex, the $\nu$(C=C) band was shifted to 1558 $cm^{-1}$ (see Table 3). The characteristic peaks of ring vibration and ring breathing for pure D- Trp were at 1232 $cm^{-1}$ and 1119 $cm^{-1}$, respectively. After the inclusion of D-Trp to b-CD, the characteristic peaks are shifted to 1233 $cm^{-1}$ and 1120 $cm^{-1}$, respectively (see, Table3).

Table 3 summarizes the $\nu$(C=C), ring vibration and ring breathing of the indole site of the pure L-, D-Trp, and b-CD inclusion complexes. The characteristic phenyl $\nu$(C=C) ring vibration and ring breathing peaks in D-Trp-b-CD were shifted to a higher wave number than that of pure D-Trp, whereas the characteristic peaks with phenyl $\nu$(C=C) ring vibration and ring breathing of the

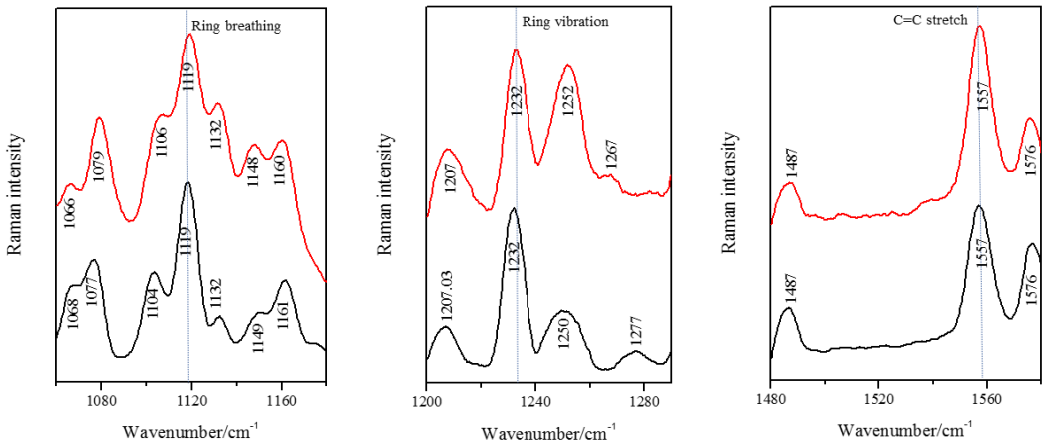


Fig. 5. Raman spectra of L-Trp (black line) and L-Trp-$\beta$-CD inclusion complexes (red line).

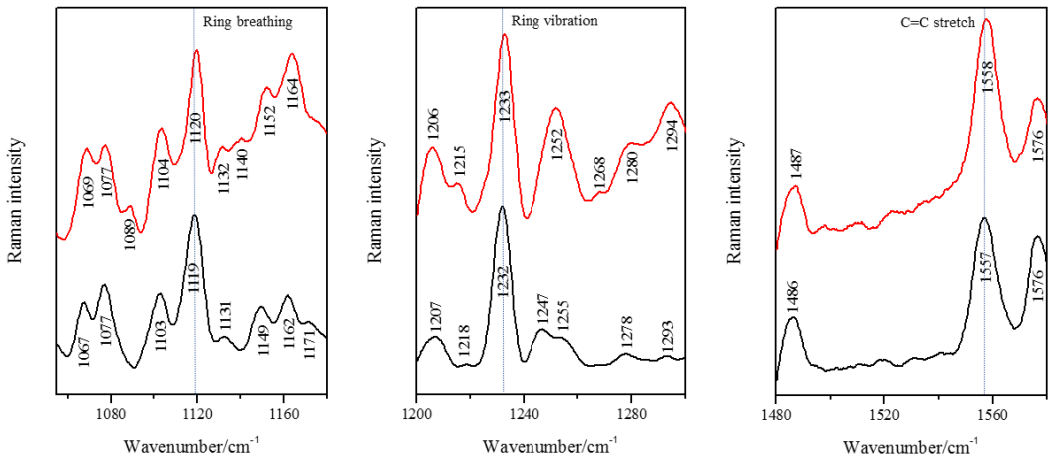


Fig. 6. Raman spectra of D-Trp (black line) and D-Trp-$\beta$-CD inclusion complexes (red line).

Table 3. Raman spectroscopy analysis for pure L-Trp and D-Trp and β-CD inclusion complexes

| | Raman peak ($cm^{-1}$) | | Raman peak ($cm^{-1}$) | | Δ($cm^{-1}$) = inclusion complex - Trp | |
|---|---|---|---|---|---|---|
| | L-Trp | D-Trp | L-Trp-β-CD | D-Trp-β-CD | L-Trp | D-Trp |
| **Ring breathing** | 1119 | 1119 | 1119 | 1120 | 0 | **1** |
| **Ring vibration** | 1232 | 1232 | 1232 | 1233 | 0 | **1** |
| **C=C stretch** | 1557 | 1557 | 1557 | 1558 | 0 | **1** |

L-Trp-b-CD inclusion complexes were not shifted to high wave number in FT-Raman spectroscopy.

## 4. Conclusions

Electrochemical and FT-Raman spectroscopic analysis were performed for D- and L-tryptophan (Trp)-*b*-cyclodextrin (CD) inclusion complex to confirm the chiral detection. We observed the higher value of the selectivity coefficient ($K_{DL}$) of the b-CD inclusion complexes than the pure D- and L-Trp in PBS solution by CV. The percentage of enantioselectivity ($I_{\%ee}$) for peak current of D-Trp-b-CD inclusion complexes was found higher than that of L-Trp-b-CD inclusion complexes. The phenyl $\nu$(C=C) stretch, ring vibration, and ring breathing for D-Try-b-CD inclusion complex showed higher chemical shifts than the L-Trp-b-CD inclusion complex.

## Acknowledgments

This work was supported by the Hannam University Research Fund (2015).

## References

1. E. Yashima and K. Maeda, Chirality-Responsive Helical Polymers, *Macromolecules*, 41, 3 (2008).
2. T. Q. Yan and C. Orihuela, Rapid and high throughput separation technologies—Steady state recycling and supercritical fluid chromatography for chiral resolution of pharmaceutical intermediates, *J. Chromatogr. A*, 1156, 220 (2007).
3. L. Zhang, M. Song, Q. Tian, and S. Min, Chiral separation of l,d-tyrosine and l,d-tryptophan by ct DNA, *Sep. Purif. Technol.*, 55, 388 (2007).
4. Z.-X. Zheng, J.-M. Lin, and F. Qu, Chiral separation of underivatized and dansyl amino acids by ligand-exchange micellar electrokinetic capillary chromatography using a copper(II)-L-valine complex as selector, *J. Chromatogr. A*, 1007, 189 (2003).
5. X. Lu, Y. Chen, L. Guo, and Y. Yang, Chiral separation of underivatized amino acids by ligand-exchange capillary electrophoresis using a copper(II)-L-lysine complex as selector, *J. Chromatogr. A*, 945, 249 (2002).
6. Elek, D. Mangelings, T. Iv´anyi, I. L´az´ar, and Y. V. Heyden,

Enantioselective capillary electrophoretic separation of tryptophane- and tyrosine-methylesters in a dual system with a tetra-oxadiaza-crown-ether derivative and a cyclodextrin, *J. J. Pharm. Biomed. Anal.*, 38, 601 (2005).
7. L. Qi, G. Yangd, H. Zhang, and J. Qiao, A chiral ligand exchange CE essay with zinc(II)-l-valine complex for determining enzyme kinetic constant of l-amino acid oxidase, *Talanta*, 81,1554 (2010).
8. L. Chi, J. Zhao, and T. D. James, Chiral mono boronic acid as fluorescent enantioselective sensor for mono α-hydroxyl carboxylic acids, *J. Org. Chem.*, 73, 4684 (2008).
9. Chiral discrimination between d- and l-tryptophan based on the alteration of the fluorescence lifetimes by the chiral additives, Yanli Wei, Sufang Wang, Shaomin Shuang, and Chuan Dong, Talanta, 81, 1800-1805 (2010).
10. F. Liu, X. Liu, S.-C. Ng, and H. S.-O. Chan, Enantioselective molecular imprinting polymer coated QCM for the recognition of l-tryptophan, *Sens. Actuators B*, 113, 234 (2006).
11. H.-S. Guoa, J.-M. Kim, S.-M. Chang, and W.-S. Kim, Chiral recognition of mandelic acid by l-phenylalanine-modified sensor using quartz crystal microbalance, *Biosens. Bioelectron.*, 24, 2931 (2009).
12. T. Stalina, K. Srinivasana, K. Sivakumar, and S. Radhakrishnan, Preparation and characterizations of solid/aqueous phases inclusioncomplex of 2,4-dinitroaniline with b-cyclodextrin, *Carbohydr. Polym.*, 107, 72 (2014).
13. N. Rajendiran, G. Venkatesh, and R.K. Sankaranarayanan, Encapsulation of thiazolyazoresorcinol and thiazolyazocresol dyes with a- and b-cyclodextrin cavities: Spectral and molecular modeling studies, *J. Mol. Struct.*, 1072, 242 (2014).
14. J. Szejtli, Introduction and General Overview of Cyclodextrin Chemistry, *Chem. Rev.*, 98, 1743 (1998).
15. A. D. Bani-Yaseen and A. Mo'ala, Spectral, thermal, and molecular modeling studies on the encapsulation of selected sulfonamide drugs in b-cyclodextrin nano-cavity, *Spectrochim. Acta, Part A*, 131, 424 (2014).
16. Z. Li, S. Chen, Z. Gu, J. Chen and J. Wu, Alpha-cyclodextrin: Enzymatic production and food applications, *Trends Food Sci. Technol.*, 35, 151 (2014).
17. W. Misiuk and M. Zalewska, Spectroscopic investigations on the inclusion interaction between hydroxypropyl-β-cyclodextrin and bupropion, *J. Mol. Liq.*, 159, 220 (2011).
18. C. Jullian, J. Morales-Montecinos, G. Zapata-Torres, B. Aguilera, J. Rodriguez, V. Ara´n, and C. Olea-Azar, Characterization, phase-solubility, and molecular modeling of inclusion complex of 5-nitroindazole derivative with cyclodextrins, Bioorg. *Med. Chem.*, 16, 5078 (2008).
19. S.-H. Choi, E.-N. Ryu, J. J. Ryoo, and K.-P. Lee, FT-Raman Spectra of o-, m-, and p-Nitrophenol Included in Cyclodextrins, *J. Inclusion Phenom. Macrocyclic Chem.*, 40, 271 (2001).
20. S.-H. Choi, S.-Y. Kim, J. J. Ryoo, and K.-P. Lee, Complexation of the Non-steroidal Anti-inflammatory Drug Loxoprofen with Modified and Unmodified β-Cyclodextrins, *J. Inclusion Phenom. Macrocyclic Chem.*, 40, 139 (2001).
21. S.-H. Choi, J.-W. Seo, S.-I. Nam, M.-S. Lee, and K.-P. Lee, FT-Raman Spectra of 2-, 3-, and 4-Chlorostyrene Molecules Included in Cyclodextrins, *J. Inclusion Phenom. Macrocyclic Chem.*, 40, 279 (2001).
22. G. qing, T. Sun, Z. Cehn, X. Yang, X. Wu, and Y. He, 'Naked-Eye' Enantioselective Chemosensors for N-Protected Amino Acid Anions Bearing Thiourea Units, *Chirality*, 21, 363 (2009).

23. S.-Z. Kang, H. Chen, X. Li, and J. Mu, Preparation of l-alanine ethyl ester modified multiwalled carbon nanotubes and their chiral discrimination between d- and l-tryptophan, *Diamond Relat. Mater.*, 19, 1221 (2010).
24. J.-B. Raoof, R. Ojani, and H. Karimi-Maleh, Carbon Paste Electrode Incorporating 1-[4-(Ferrocenyl Ethynyl) Phenyl]-1-Ethanone for Electrocatalytic and Voltammetric Determination of Tryptophan, *Electroanalysis*, 20, 1259 (2008).
25. G. K. Budnikov, G. A. Evtyugin, Y. G. Budnikova, and V. A. Al'fonsov, Chemically modified electrodes with amperometric response in enantioselective analysis, *Journal of Analytical Chemistry*, 63, 2 (2008).